

# Microtubule Alterations and Mutations Induced by Desoxyepothilone B: Implications for Drug-Target Interactions

Nicole M. Verrills,<sup>1,2</sup> Claudia L. Flemming,<sup>1</sup> Marjorie Liu,<sup>1</sup> Michael T. Ivery,<sup>3</sup> Gary S. Cobon,<sup>2</sup> Murray D. Norris,<sup>1</sup> Michelle Haber,<sup>1</sup> and Maria Kavallaris<sup>1,\*</sup>

<sup>1</sup>Children's Cancer Institute Australia for Medical Research

Randwick, New South Wales, 2031

<sup>2</sup>Australian Proteome Analysis Facility Macquarie University

Sydney, New South Wales, 2109

<sup>3</sup>Faculty of Pharmacy

University of Sydney

Sydney, New South Wales, 2006

Australia

## Summary

Epothilones, like paclitaxel, bind to  $\beta$ -tubulin and stabilize microtubules. We selected a series of four leukemia sublines that display increasing levels of resistance to the epothilone analog desoxyepothilone B (dEpoB). The dEpoB cells selected in 30–140 nM were  $\sim$ 15-fold cross-resistant to paclitaxel, while 300 nM selected cells were 467-fold resistant to this agent. The dEpoB-selected cells are hypersensitive to microtubule destabilizing agents, and express increased levels of class III  $\beta$ -tubulin and MAP4. A novel class I  $\beta$ -tubulin mutation, A231T, that affects microtubule stability but does not alter paclitaxel binding, was identified. The 300 nM selected cells acquired a second mutation, Q292E, situated near the M loop of class I  $\beta$ -tubulin. These cells fail to undergo drug-induced tubulin polymerization due to dramatically reduced drug binding. The dEpoB-resistant leukemia cells provide novel insights into microtubule dynamics and, in particular, drug-target interactions.

## Introduction

Natural product antimitotic drugs targeting the tubulin/microtubule system are important in the treatment of a range of haematologic and solid cancers. One of these agents, paclitaxel (Taxol), is used in the treatment of a variety of tumor types including lung, ovarian, and breast cancer [1]. Paclitaxel induces its effect through its ability to bind to the tubulin dimer at the core of the microtubule structure [2] and disrupts the tubulin-microtubule equilibrium by stabilizing the polymerized form [3]. Agents such as paclitaxel are believed to exert their cytotoxic effect by interfering with the function of the mitotic spindle, blocking cells at the metaphase/anaphase junction of mitosis [4].

Recently, new agents with similar microtubule stabilizing effects to paclitaxel have been identified [5, 6]. Among the most promising class of new agents are the

epothilones which were originally identified in myxobacterium *S. cellulosum* and are structurally distinct from the taxanes. Bollag et al. [7] isolated epothilone A and B which belong to the 16-membered macrolide antibiotic family of compounds. In vitro, epothilones induce the polymerization of tubulin dimers into microtubules and can stabilize preformed microtubules against depolymerization [7, 8]. Mutational and pharmacophore analyses indicate a common binding site between paclitaxel and the epothilones [9–12], and indeed these compounds competitively inhibit [<sup>3</sup>H]-paclitaxel binding to microtubules [7, 8]. As with paclitaxel, epothilones arrest cells at the G<sub>2</sub>M transition of the cell cycle leading to cell death; however, unlike paclitaxel, the epothilones retain cytotoxicity in P-glycoprotein-expressing multidrug-resistant (MDR) cells [7, 8, 12, 13]. In vivo, EpoA and EpoB showed only moderate antitumor activity due to a narrow therapeutic window [14, 15]; however, phase I clinical trials of EpoB, and a synthetic analog, BMS-247550, are encouraging [16]. A recently developed EpoB analog, Z-12,13-desoxyepothilone B (dEpoB), has shown very promising in vivo activity [13, 14, 17]. While less potent than EpoB in vitro, a comparative study showed dEpoB to have the least cross-resistance compared to epothilones A, B, and dEpoA in numerous drug-resistant cancer cell lines [13]. dEpoB also showed the greatest therapeutic effect in xenograft models, including mice bearing doxorubicin-resistant human mammary adenocarcinoma xenografts and MDR human lymphoblastic T cell leukemia (CCRF-CEM/paclitaxel) [13, 14]. In a more extensive study, dEpoB showed variable efficacy compared to paclitaxel in a panel of human xenografts; however, in all drug-resistant tumors analyzed, dEpoB showed the greatest therapeutic effect [17].

To enhance understanding of the drug-target interactions of dEpoB, and to identify resistance mechanism(s) to aid in future drug design of related agents, we have selected a series of human T cell acute lymphoblastic leukemia (ALL) cells, CCRF-CEM, for resistance to dEpoB. Stepwise selection in dEpoB resulted in four cell lines with increasing resistance to the selecting agent that display cross-resistance to microtubule-stabilizing agents and hypersensitivity to microtubule-destabilizing agents. The resistant cells initially acquired a mutation in  $\beta$ -tubulin that resulted in reduced microtubule stability counteracting the effects of microtubule stabilizing agents. In the highly resistant subline, the cells acquired a second mutation that resulted in reduced drug binding. This study provides novel insights into microtubule stability and, in particular, drug-target interactions.

## Results

### Resistance Profiles of dEpoB-Selected Leukemia Cells

Selection of CCRF-CEM leukemia cells with increasing concentrations of dEpoB resulted in the derivation of

\*Correspondence: [m.kavallaris@unsw.edu.au](mailto:m.kavallaris@unsw.edu.au)

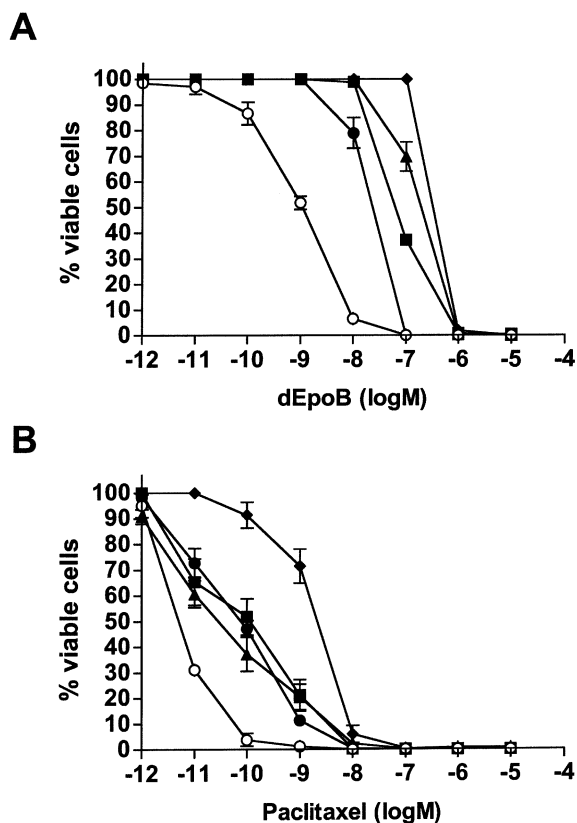


Figure 1. Resistance Profiles with the Selecting Agent, dEpoB, and Paclitaxel

(A) The dEpoB30, dEpoB60, dEpoB140, and dEpoB300 cells display increasing resistance to dEpoB, respectively.

(B) The dEpoB30, dEpoB60, and dEpoB140 cells all show similar levels of cross-resistance to paclitaxel. The dEpoB300 cells show much higher cross-resistance to this drug. Cytotoxicity assays were performed on the CEM (open circles), dEpoB30 (closed circles), dEpoB60 (closed squares), dEpoB140 (closed triangles), and dEpoB300 (closed diamonds) cell lines as described in Experimental Procedures. All assays were run with four replicates at eight concentrations of drug. Bars,  $\pm$ SE of three individual experiments.

four sublines, designated CEM/dEpoB30, CEM/dEpoB60, CEM/dEpoB140, and CEM/dEpoB300. The resultant sublines are 21-, 60-, 173-, and 307-fold resistant to dEpoB respectively, compared to parental CEM cells (Figure 1A; Table 1). The dEpoB-resistant cells also dis-

play cross-resistance to paclitaxel; however, the extent of resistance in the dEpoB300 cells is far greater than in any of the other cell lines and is also greater than the fold resistance to the selecting agent, dEpoB (Figure 1B; Table 1). Resistance to the related drug, EpoB, was less than that to the selecting agent (Table 1). Analysis of growth rates showed that the dEpoB-resistant cells have a slightly reduced doubling time (CEM, 22.3 hr; dEpoB30, 18.6 hr; dEpoB60, 17.6 hr; dEpoB140, 20.5 hr; dEpoB300, 20.4 hr; data not shown), and none of the cell lines are dependent on dEpoB for growth.

Interestingly, dEpoB-resistant cell lines are hypersensitive to *vinca* alkaloids which destabilize microtubules (Table 1). The dEpoB30 cell line shows the broadest sensitivity to *vinca* alkaloids, being hypersensitive to vincristine, vinblastine, and vinorelbine. The dEpoB300 cells are hypersensitive to vinblastine and vinflunine with a trend toward hypersensitivity to vinorelbine, while the dEpoB60 cells are hypersensitive only to vinblastine. No significant cross-resistance was observed to the DNA binding agent doxorubicin in any of the dEpoB-selected sublines.

#### Resistance Is Not Due to Increased *MDR1* or *MRP1* Expression

P-glycoprotein (encoded by the *MDR1* gene) and the multidrug-resistance associated protein 1 (encoded by the *MRP1* gene) are membrane transporters associated with the MDR phenotype. Semiquantitative competitive RT-PCR showed that expression of the *MDR1* and *MRP1* genes were not upregulated in the dEpoB-resistant cell lines (Supplementary Figures S1A and S1B at <http://www.chembiol.com/cgi/content/full/10/7/597/DC1>). To determine whether decreased drug accumulation was contributing to resistance, accumulation of [<sup>3</sup>H]-paclitaxel was analyzed. No reduction in [<sup>3</sup>H]-paclitaxel accumulation was observed in the dEpoB-resistant cells (Supplementary Figure S1C at <http://www.chembiol.com/cgi/content/full/10/7/597/DC1>). These results suggest that the resistance profile of the dEpoB cells is not attributable to decreased drug accumulation.

#### Altered Tubulin and MAP4 Expression in dEpoB-Resistant Cells

Previous studies have identified altered expression of specific tubulin isotypes and microtubule-associated proteins (MAPs) in association with antimicrotubule

Table 1. Resistance of CEM/dEpoB-Selected Cells

| Cell Line | Relative Resistance <sup>a</sup> |      |       |      |       |       |       |      |     |
|-----------|----------------------------------|------|-------|------|-------|-------|-------|------|-----|
|           | dEpoB                            | EpoB | Ptx   | VCR  | VLB   | VNFL  | VNRL  | COLC | DOX |
| dEpoB30   | 21**                             | NT   | 16**  | 0.6* | 0.28* | 0.82  | 0.43* | 0.78 | 1.4 |
| dEpoB60   | 60**                             | NT   | 26**  | 1.5  | 0.58* | 0.73  | 0.94  | 0.88 | 1.8 |
| dEpoB140  | 173**                            | 12** | 7*    | 2.3  | 0.79  | 0.86  | 1.31  | 0.88 | 2.2 |
| dEpoB300  | 307**                            | 77** | 467** | 1.3  | 0.25* | 0.52* | 0.59  | 0.85 | 1.1 |

\*p < 0.05; \*\*p < 0.005. The IC<sub>50</sub> values (Log M)  $\pm$  SE of the parent CEM cells are as follows: dEpoB,  $1.07 \times 10^{-9} \pm 0.055$ ; EpoB,  $4.66 \times 10^{-10} \pm 0.023$ ; Ptx,  $4.50 \times 10^{-12} \pm 0.048$ ; VCR,  $2.26 \times 10^{-10} \pm 0.060$ ; VLB,  $4.29 \times 10^{-9} \pm 0.075$ ; VNFL,  $3.16 \times 10^{-8} \pm 0.005$ ; VNRL,  $2.49 \times 10^{-9} \pm 0.067$ ; COLC,  $3.66 \times 10^{-9} \pm 0.064$ ; and DOX,  $1.26 \times 10^{-9} \pm 0.501$ .

Abbreviations: dEpoB, desoxyepothilone B; EpoB, epothilone B; Ptx, paclitaxel; VCR, vincristine; VLB, vinblastine; VNFL, vinflunine; VNRL, vinorelbine; COLC, colchicine; DOX, doxorubicin; and NT, not tested.

<sup>a</sup>Determined by dividing the IC<sub>50</sub> for the resistant cell line by the IC<sub>50</sub> of the parent (CEM) cell line.

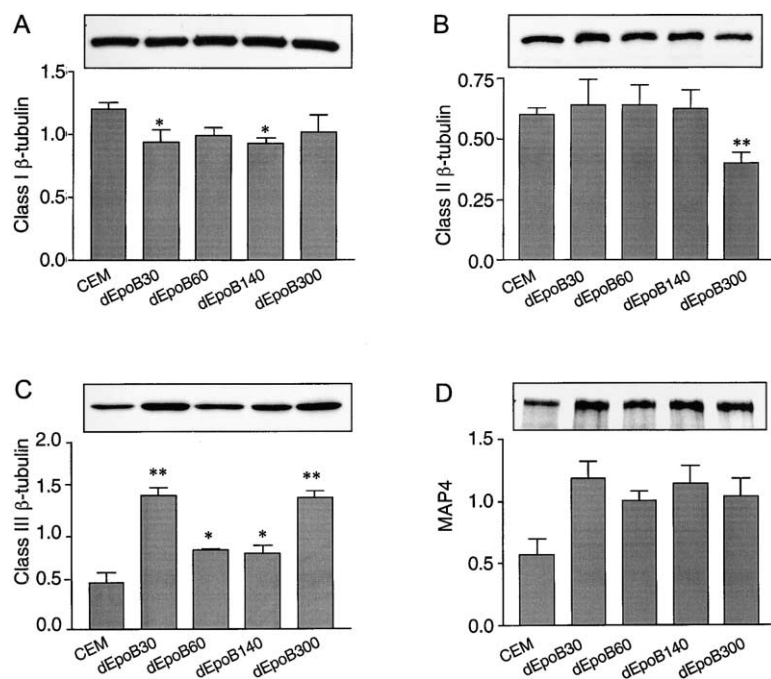


Figure 2. Altered Protein Expression of Tubulin and MAP4

Total cellular protein (10  $\mu$ g) from CEM (lane 1), dEpoB30 (lane 2), dEpoB60 (lane 3), dEpoB140 (lane 4), and dEpoB300 (lane 5) was separated on 4%–15% SDS-PAGE, electrotransferred to nitrocellulose, and immunodetected with antibodies against class I  $\beta$ -tubulin (A); class II  $\beta$ -tubulin (B); class III  $\beta$ -tubulin (C); and MAP4 (D). Membranes were stripped and reprobed with actin. Inset panel above each graph is a representative blot of four independent experiments. The relative expression of each protein was determined by dividing the densitometric value of the test protein by that of the actin control. Bars,  $\pm$ SE of four experiments; \* $p$  < 0.05; \*\* $p$  < 0.005.

drug resistance [18–20]. To analyze the protein expression in dEpoB-resistant cells, Western blots were performed (Figure 2). All dEpoB-resistant cells have slightly reduced expression of class I  $\beta$ -tubulin (Figure 2A), and class II  $\beta$ -tubulin is reduced only in the dEpoB300 cells (Figure 2B). In contrast, class III  $\beta$ -tubulin, a protein previously shown to be upregulated in cells resistant to microtubule-stabilizing agents, and downregulated in cells resistant to microtubule-destabilizing drugs (reviewed in [19, 20]), showed increased expression in all dEpoB-resistant cells. dEpoB30 and dEpoB300 cells had the greatest increase in this isotype (approximately 3-fold) compared to the parental CCRF-CEM cells (Figure 2C). Interestingly the dEpoB30 and dEpoB300 sublines also displayed the broadest hypersensitivity to *vinca* alkaloids (Table 1). No significant change in total  $\alpha$ -tubulin was observed (data not shown). Modification of MAP4 expression can lead to altered efficacy of antimicrotubule agents [21, 22], and expression of this MAP was increased approximately 2-fold in all dEpoB-resistant cells (Figure 2D).

#### dEpoB-Resistant Cells Have Reduced Intrinsic and Drug-Induced Polymerized Tubulin

To assess the capacity of tubulin to form stable microtubules in the resistant sublines, soluble and polymerized pools of tubulin were separated from cell lysates and the relative proportions determined by Western blotting. The dEpoB-resistant cells have greatly reduced amounts of polymerized tubulin compared to the CEM cells (Figure 3). The percentage of polymerized tubulin is 27.5% in the parental CEM cells, and 17.5%, 13.4%, 9.3%, and 6.9% in the dEpoB30, dEpoB60, dEpoB140, and dEpoB300 cells respectively (Figure 3B). Thus, the relative levels of polymerized tubulin decreases as the extent of dEpoB resistance increases. To determine if the tubulin in these cells could be induced to polymerize by

dEpoB, drug was introduced to the cell lysis buffer. The parental cells show significant increases in polymerized tubulin with 4  $\mu$ g/ml dEpoB (Figure 3). At 4  $\mu$ g/ml dEpoB, the proportional increase in polymerized tubulin in the dEpoB30-140 cells is similar to the parental CEM cells. It must be noted, however, that as intrinsic levels were lower in all the resistant cells, the overall amounts of polymerized tubulin still remained less than in the CEM cells. In contrast, addition of dEpoB to the dEpoB300 cells failed to induce tubulin polymerization.

#### dEpoB300 Cells Have Impaired Paclitaxel Binding

To determine whether the lack of drug-induced tubulin polymerization is due directly to reduced drug binding to microtubules, cells were treated with [ $^3$ H]-paclitaxel for 1 hr prior to separation of soluble and polymerized fractions of tubulin. The total [ $^3$ H]-paclitaxel was determined relative to the total protein in each polymerized fraction (Figure 4). The dEpoB30-140 cells bound the same amount of [ $^3$ H]-paclitaxel as the parental CEM cells. In contrast, dEpoB300 cells bound less than half that amount compared to CEM cells ( $p$  < 0.0001). Thus, the dEpoB300 cells have greatly reduced binding efficiency for [ $^3$ H]-paclitaxel compared to the drug-sensitive parental cells.

#### dEpoB-Resistant Cells Have Mutations in HM40 (Class I) $\beta$ -Tubulin

To determine if reduced polymerized tubulin levels were due to mutations in tubulin, the predominant  $\beta$ -tubulin isotype gene, HM40 (encodes class I  $\beta$ -tubulin), was sequenced in the dEpoB-selected cells. A heterozygous point mutation at nucleotide 691 (GCC  $\rightarrow$  ACC), resulting in an alanine to threonine substitution at amino acid 231 was observed in all dEpoB-resistant cell lines. A second heterozygous point mutation at nucleotide 874 (CAG  $\rightarrow$  GAG), substituting a glutamine to glutamic acid at amino

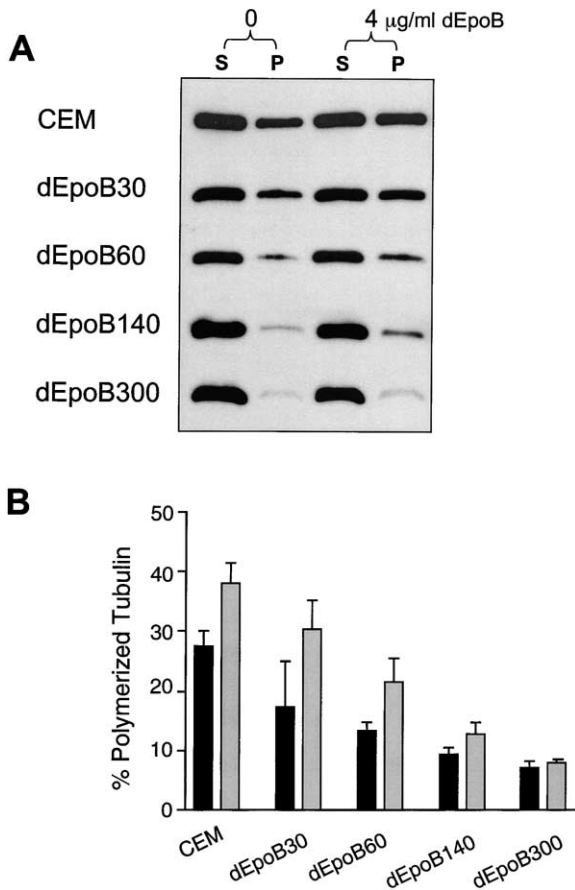


Figure 3. Decreased Polymerized Tubulin and Reduced Drug-Induced Polymerization in dEpoB-Resistant Cells

(A) Soluble and polymerized pools of tubulin were separated in the absence or presence of 4  $\mu\text{g/ml}$  dEpoB in the lysis buffer, and relative amounts determined by Western blotting with a mAb to total  $\alpha$ -tubulin.

(B) The percent polymerized tubulin was calculated by dividing the polymerized fraction (P) by the total polymerized and soluble fractions (P + S), and values are  $\pm$ SE for three individual experiments. S, soluble; P, polymerized. Analysis of variance was calculated for each dEpoB value compared to the parental CEM cells. Bars,  $\pm$ SE.

acid 292 was found in the dEpoB140 and dEpoB300 cells. Interestingly, the wild-type base at this position in the dEpoB140 cells predominated over the mutant, while in the dEpoB300 cells, the mutant sequence predominated (data not shown), indicating that this mutation occurred in the late stages of the dEpoB140 selection, and gave a selective advantage over the wild-type in the dEpoB300 selection.

#### Class I $\beta$ -Tubulin Mutations Are Expressed at the Protein Level

To ensure that the mutations identified in the HM40 gene are translated and expressed at the protein level, cellular proteins were separated by 2D-PAGE and tubulin tryptic peptides analyzed by mass spectrometry (MS) (Figures 5A and 5B). Spots 1 and 3 were identified by MALDI-TOF MS peptide mass fingerprinting and Western blotting as class II  $\beta$ -tubulin, and spots 2 and 4 as class I  $\beta$ -tubulin

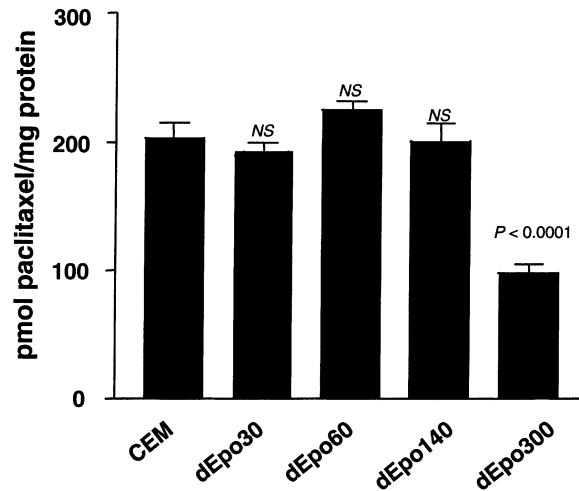


Figure 4. dEpoB-Resistant Cells Display Reduced [ $^3\text{H}$ ]-Paclitaxel Binding

Cells were incubated in the presence of [ $^3\text{H}$ ]-paclitaxel for 60 min prior to separating the soluble and polymerized pools of tubulin as described in Experimental Procedures. The amount of [ $^3\text{H}$ ]-paclitaxel in the polymerized fraction was determined and the results expressed as pmol paclitaxel/mg protein. Analysis of variance was calculated for each dEpoB value compared to the parental CEM cells. Bars,  $\pm$ SE.

(data not shown). Analysis of the tryptic peptide spectrum of class I  $\beta$ -tubulin spot 2 identified one peptide of different mass in the parental CEM cells and the dEpoB-resistant cells (data not shown). The ion at 908.32 in the CEM cells corresponds to the  $\text{H}^{3+}$  tryptic peptide of amino acids 217–241. In the dEpoB140 cells, this peptide is replaced by a  $\text{H}^{3+}$  ion at 918.31, a relative increase of 30 Da. Upon tandem MS and amino acid sequence analysis, 14 amino acids could be called and the sequence of these two peptides was found to be HLVSATMSGVTTCL and HLVSITMSGVTTCL respectively (Figures 5Aii and 5Aiii). Thus, the increase in 30 Da is due to the substitution of an alanine for a threonine at position 231 in the dEpoB-resistant cells. The point mutation at nucleotide 691 identified in the HM40 gene is therefore translated and expressed at the protein level.

Similarly, the Q292E mutation observed in the HM40 gene sequence is expressed at the protein level in the dEpoB300 cells (Figure 5B). In this case, the MALDI-TOF spectra showed a 1660.99 Da peptide in the CEM cells, substituted by a peptide at 1661.98 Da in the dEpoB300 cells. ESI-TOF MS/MS on this peptide identified the sequence as TVPELTQQVFDK and TVPELTQE $\text{V}$ FDK (amino acids 285–297) in the CEM and dEpoB300 cells respectively, and thus the mutation of glutamine to glutamic acid is also present at the protein level (Figure 5Biii). Expression of the Q292E mutation was only observed at the protein level in the dEpoB300 cells. This amino acid substitution results in the gain of an acidic residue, hence decreasing the isoelectric point of the protein causing it to migrate to a more acidic region in the 2D gel. The mutated polypeptide is now migrating directly underneath the class II  $\beta$ -tubulin spot 3 (Figure 5Bi). Spot 3 was analyzed by peptide mass fingerprinting and MS/MS to confirm that the peptide

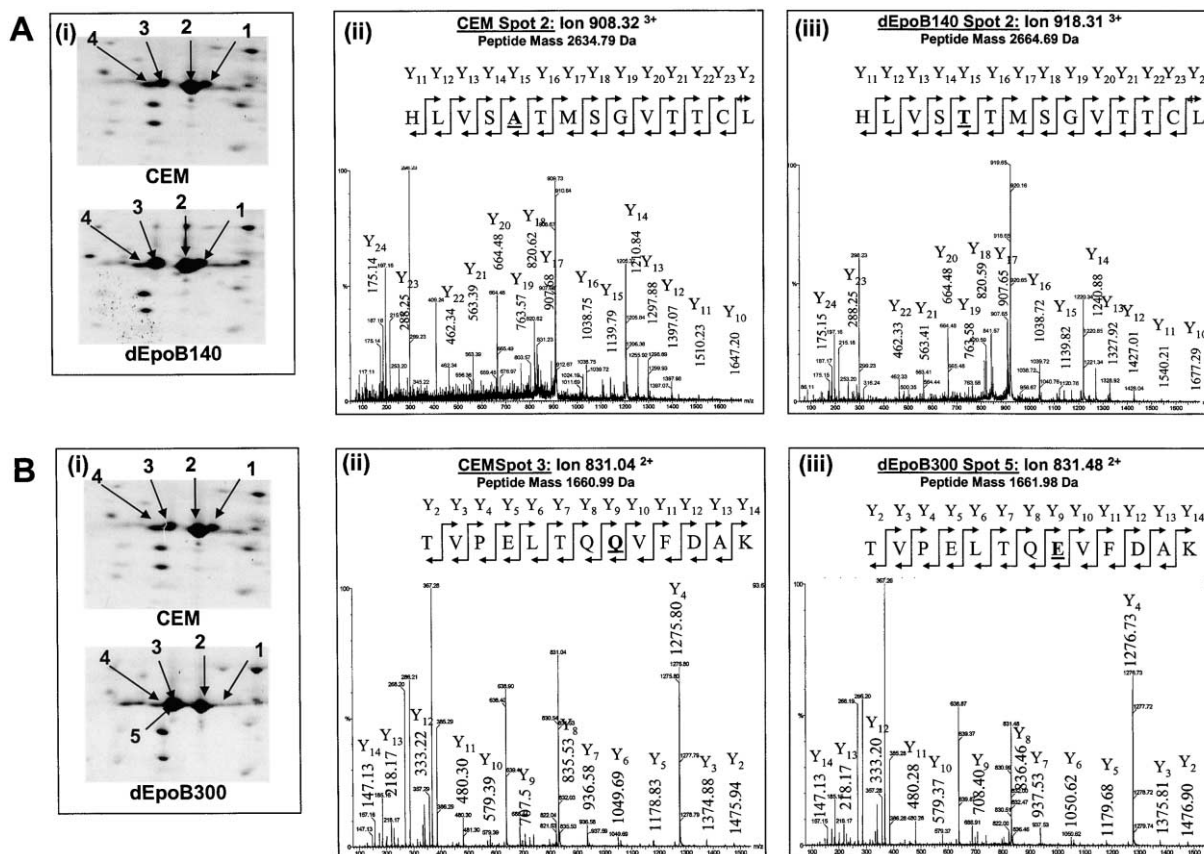


Figure 5. Mutations in Class I  $\beta$ -Tubulin Are Expressed at the Protein Level

(Ai) Cellular proteins from CEM and dEpoB140 cells were separated by 2D-PAGE and stained with SYPRO Ruby. Tubulin spots were excised from the gel, in-gel trypsin digested, and resulting peptides analyzed by MALDI-TOF MS. Spots 1 and 3 were identified as class II  $\beta$ -tubulin and spots 2 and 4 as class I  $\beta$ -tubulin. Spectra were compared for each protein in the CEM, and dEpoB140 cells and peptides differing in mass were selected for tandem mass spectrometry (MS/MS).

(Aii) ESI-TOF MS/MS spectrum of peptide with mass 2634.79 Da (ion 908.32<sup>3+</sup>) from the CEM cells.

(Aiii) ESI-TOF MS/MS spectrum of peptide with mass 2664.69 Da (ion 918.31<sup>3+</sup>) from the dEpoB140 cells.

(Bi) Cellular proteins from CEM and dEpoB300 cells were separated by 2D-PAGE and stained with SYPRO Ruby. Tubulin spots were excised from the gel, in-gel trypsin digested, and resulting peptides analyzed by MALDI-TOF MS. Spots 1 and 3 were identified as class II  $\beta$ -tubulin and spots 2, 4, and 5 as class I  $\beta$ -tubulin. Spectra were compared for each protein in the CEM and dEpoB300 cells, and peptides differing in mass were selected for tandem mass spectrometry (MS/MS).

(Bii) ESI-TOF MS/MS spectrum of peptide at mass 1660.99 Da from the CEM cells.

(Biii) ESI-TOF MS/MS spectrum of peptide at mass 1661.98 Da from the dEpoB300 cells. ESI-TOF MS/MS data was manually analyzed to determine the amino acid sequence of selected peptides.

shift and Q292E mutation was seen only in the lower, class I  $\beta$ -tubulin spot (Figure 5Bi, dEpoB300 spot 5). In addition to the mutations identified, 2D-PAGE analysis shows the loss of a class II  $\beta$ -tubulin protein spot in the dEpoB300 cells (Figure 5Bi, spot 1). This finding corresponds to the reduced class II  $\beta$ -tubulin expression observed in these cells by Western blotting (Figure 2B).

#### Mutations in $\beta$ -Tubulin Map to H7 in the Drug Binding Site and H9 Near the M Loop

An increasingly well-resolved model for the  $\alpha/\beta$  tubulin dimer has been obtained through the application of electron crystallography to zinc induced paclitaxel-tubulin sheets [23]. A ribboned diagram for the  $\beta$ -tubulin monomer as deposited in the Protein Data Bank (PDB: 1JFF) is illustrated in Figure 6, which shows paclitaxel binding in a very large binding site lying between the M and

S9–S10 loops and bounded by helices H6 and H7. This region of  $\beta$ -tubulin is thought to play an important role in the formation of lateral contacts between protofilaments [24]. Molecular modeling studies have positioned the A231T and Q292E mutations in  $\beta$ -tubulin. The novel A231T mutation resides on helix 7 (H7) of  $\beta$ -tubulin (Figure 6), which has previously been defined as part of the paclitaxel binding site [25] and is also a region implicated in controlling the conformation of the tubulin molecule [26, 27]. The second  $\beta$ -tubulin mutation, Q292E, is located on H9 near the M loop (Figure 6), a region important in the interactions between protofilaments.

#### Discussion

The EpoB analog Z-12,13-desoxyepothilone B (dEpoB) displays promising *in vivo* activity, and only low-level

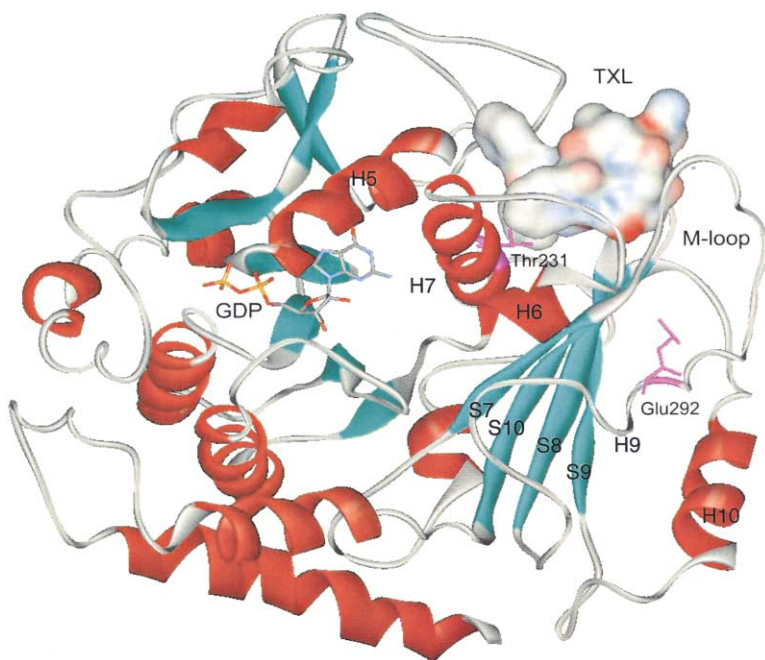


Figure 6. Modeling of the A231T and Q292E Mutations in  $\beta$ -Tubulin

The molecular structure of the  $\alpha/\beta$ -tubulin heterodimer has recently been determined (PDB: 1JFF). This figure shows paclitaxel binding in a very large binding site lying between the M and S9–S10 loops and bounded by helices H6 and H7. The A231T mutation identified in all the dEpoB-resistant cell lines is located on H7 within the paclitaxel binding site. The Q292E mutation identified in the dEpoB300 cells is situated on H9 near the edge of the M loop, a region implicated in lateral contacts of protofilaments and paclitaxel binding.

resistance to dEpoB has previously been achieved in culture [17]. An important benefit of the epothilones over existing antimicrotubule agents such as paclitaxel is primarily due to the ability of these agents to retain cytotoxicity against MDR cells [7, 8]. This study describes the selection and characterization of dEpoB-resistant human ALL cells (CCRF-CEM) in which reduced drug accumulation and the MDR-phenotype is not involved in the resistance phenotype. The major mechanism identified is associated with modifications in the tubulin/microtubule system, the target of dEpoB, and other antimicrotubule agents. Tubulin/microtubule alterations include altered tubulin isotype expression and increased levels of MAP4. The increased MAP4 expression is most likely compensating for the reduced microtubule stability induced by the acquired  $\beta$ -tubulin mutations. Importantly, the reduced efficacy of microtubule-stabilizing agents in these cells was found to be due to either decreased microtubule stability or a defect in drug binding.

Epothilones share a similar mechanism of action with paclitaxel [7, 8]. The effects of paclitaxel on microtubule dynamics have been extensively studied. At low concentrations paclitaxel strongly suppresses microtubule dynamics [4, 28], and at higher concentrations significantly increases the microtubule polymer mass and induces microtubule bundle formation [3, 28]. Studies on paclitaxel-resistant cells indicate that resistance may be associated with impaired tubulin polymerization [12, 29]. All the dEpoB-resistant cell lines studied here have greatly reduced tubulin polymer mass. In addition, the reduction in polymer mass is inversely correlated to the extent of dEpoB resistance. In the dEpoB30, dEpoB60, and to a lesser extent in the dEpoB140 cells, dEpoB could induce polymerization of tubulin, although never to the same overall levels as the parental cells (Figure 3). Thus, the microtubules in these cells appear to retain

some ability to polymerize. However, the reduced initial polymer mass would render fewer microtubules available for drug binding and hence reduce drug efficacy. In contrast, dEpoB could not induce tubulin polymerization in the dEpoB300 cells.

According to the “T-paclitaxel conformation bound to  $\beta$ -tubulin model” proposed by Snyder et al. [30], the novel human class I  $\beta$ -tubulin A231T mutation identified in the dEpoB-resistant CEM cells lies in the highly hydrophobic paclitaxel binding region of  $\beta$ -tubulin. This mutation, identified by both gene and protein sequencing, leads to a change from a hydrophobic to a polar residue. The mutation resides on helix 7 (H7) of  $\beta$ -tubulin, a region implicated in microtubule stability [23, 27, 31]. As threonine is C- $\beta$  branched, it introduces more bulkiness near to the protein backbone so that the substitution of this amino acid restricts the conformations the main chain can adopt. In particular, it is more difficult for C- $\beta$ -branched amino acids to adopt an  $\alpha$ -helical conformation. We hypothesized that this mutation confers a selective survival advantage to the cells in the presence of dEpoB due to decreased stability of microtubules counteracting the drug-stabilizing effects, and/or reduced drug binding. We strongly favor the first possibility for the resistant cells harboring the A231T mutation, as the microtubules in these cells retain their ability to bind paclitaxel (Figure 4). Studies from the Cabral laboratory [32] demonstrated that mutations in a leucine-rich region of  $\beta$ -tubulin involving L215H, L217R, and L228F were also associated with reduced microtubule stability and were less sensitive to the effects of paclitaxel. The  $\beta$ -tubulin L228 residue lies deep in the hydrophobic pocket of  $\beta$ -tubulin on H7 and resides only 3 residues away from the A231T CEM-dEpoB mutation also on the same helix. These authors demonstrated that amino acid substitutions in any of these leucines perturbed the assembly of microtubules. Moreover, it

has been hypothesized that the H7 of tubulin controls the conformation of the whole molecule [26]. Our findings support and extend the observation that the H7 of  $\beta$ -tubulin plays an important role in microtubule stability. Our results indicate that reduced microtubule stability is most likely the overriding mechanism of resistance in the dEpoB30-140 cells harboring the A231T mutation. The demonstrated ability of tubulin in these cells to polymerize despite their reduced intrinsic levels of polymerized tubulin confirms that drug-induced polymerization can still occur, albeit to a reduced extent. In addition, the ability of paclitaxel to bind as effectively to microtubules in the dEpoB30-140 cells as in the parental CEM cells offers further support for reduced microtubule stability counteracting the drug effects in these cells.

In addition to the A231T mutation, the dEpoB300 cells acquired a second expressed class I  $\beta$ -tubulin mutation, Q292E, and display a reduced ability to undergo drug-induced polymerization. Thus, a glutamine at position 292 may be crucial for effective epothilone binding or alternatively, destabilization of the M loop negates the stabilizing effects of the drug. This particular mutation and amino acid substitution is of interest as it has previously been described in EpoB-selected A549 lung cancer cells that are 95-fold resistant to the selecting agent [33], a level similar to the 77-fold EpoB cross-resistance exhibited by the dEpoB300 cells. It has been implicated in the lateral contacts of the protofilaments and resides on H9 near the M loop of  $\beta$ -tubulin. It is also in close proximity to the Thr-274 residue that forms part of the paclitaxel/Epo binding pocket. Both glutamine and glutamic acid prefer to be on the surface of proteins, exposed to an aqueous environment. They are frequently involved in protein active or binding sites, with the polar side chain useful for interactions with other polar or charged atoms. However, the negative charge on glutamic acid means that this mutation would alter binding interactions at this site.

Remarkably, the dEpoB300 cells display greater cross-resistance to paclitaxel than the other dEpoB-resistant cells and to the selecting agent, dEpoB (Table 1). While paclitaxel and epothilones appear to share a common binding site, the exact conformation and residues involved in this binding are far from clear, especially for the epothilones. Thus, it is possible that the Q292E mutation affects binding of paclitaxel or the ability of paclitaxel to overcome microtubule destabilization more so than dEpoB, indicating that these drugs do not bind to the tubulin molecule in an identical manner. The demonstration that dEpoB300 cells display a significant reduction in paclitaxel binding on microtubules compared to the parent and other dEpoB-resistant cells provides direct evidence that reduced drug binding is contributing to resistance.

We cannot exclude the possibility that other microtubule changes are contributing to the increased resistance to paclitaxel and reduced microtubule binding of this drug in the dEpoB300 cells. The only change observed exclusively in the dEpoB300 cells is the downregulation of class II  $\beta$ -tubulin. Paclitaxel resistance has previously been associated with increased expression of class II  $\beta$ -tubulin [34, 35]. Thus, we would not expect the downregulation of this isotype observed in the

dEpoB300 cells to be increasing paclitaxel resistance. However, 2D-PAGE analysis demonstrates the loss of one isoform of class II  $\beta$ -tubulin, and retention of a second, more basic isoform (Figure 5B). This is usually indicative of a change in the posttranslational modification of class II  $\beta$ -tubulin in these cells. Posttranslational modifications of tubulin can increase microtubule stability (reviewed in [36–38]). We can speculate that loss of a class II  $\beta$ -tubulin modification may alter the interaction of this molecule with paclitaxel; however, specific analysis of the modification is required to determine if this isotype has any involvement in the heightened paclitaxel resistance.

Another likely factor contributing to the resistance phenotype is the high expression of class III  $\beta$ -tubulin observed in the dEpoB-resistant cells. The effect of  $\beta$ -tubulin isotype composition on microtubule assembly and antimicrotubule drug interactions *in vitro* has been previously described. Tubulin dimers consisting of  $\alpha$ -tubulin and class III  $\beta$ -tubulin are less sensitive to the suppression of microtubule dynamics by paclitaxel than  $\alpha/\beta$ -tubulin dimers enriched for other  $\beta$ -tubulin isotypes [39], and class III  $\beta$ -tubulin-depleted microtubules undergo paclitaxel-induced polymerization more readily than unfractionated tubulin [40]. Similar studies with epothilones have not been reported. Studies from our group and those of others have found increased expression of class III  $\beta$ -tubulin in paclitaxel-resistant cell lines and paclitaxel-resistant ovarian tumor samples [18–20], and downregulation of this isotype partially restores paclitaxel sensitivity [41]. Therefore, the increased class III  $\beta$ -tubulin in the dEpoB-resistant cells studied herein may be contributing to the resistance phenotype. However, it is unlikely to be the predominant mechanism of resistance, as class III  $\beta$ -tubulin expression did not increase any further after the initial dEpoB30 selection, whereas the level of polymerized tubulin decreases concurrently as resistance increases. In addition, gene sequencing and MS analysis reveals the relative proportion of the Thr<sup>231</sup> mutation over the wild-type sequence also increases from the dEpoB30 to dEpoB140 cells, and that the Glu<sup>292</sup> mutation increases from very low levels in the dEpoB140 to high levels in dEpoB300 cells (data not shown). These findings further support that the reduction in polymerized tubulin is due more to the mutations than the heightened class III expression. Interestingly though, class III  $\beta$ -tubulin expression was highest in the dEpoB30- and dEpoB300-resistant cells, and these two cells lines showed the broadest hypersensitivity to *vinca* alkaloids. Downregulation of class III  $\beta$ -tubulin has previously been associated with *vinca* alkaloid-resistant leukemia cells [42]. Thus, we propose that the high class III  $\beta$ -tubulin expression increases the efficacy of *vinca* alkaloids and decreases the effects of microtubule stabilizing agents via subtle effects on microtubule dynamics and/or drug binding, but does not affect the intrinsic levels of polymerized tubulin.

The upregulation of MAP4 in all the dEpoB-resistant cells (Figure 4) is interesting since MAP4 is a high *M<sub>r</sub>* protein that binds to and stabilizes microtubules. Modifying the expression of MAP4 via gene overexpression or antisense approaches leads to changes in microtubule stability and alterations in paclitaxel binding [21, 22, 43].

In addition, increased MAP4 expression has previously been associated with enhanced sensitivity to paclitaxel and resistance to microtubule-destabilizing agents, such as vincristine [21, 42]. Thus, it would seem counter-intuitive to increase MAP4 expression in cells resistant to a microtubule-stabilizing agent such as dEpoB. The identification of MAP4 in the polymerized tubulin fraction (data not shown) indicates that MAP4 can bind to the microtubules that are present in these cells. As the increased MAP4 expression is not resulting in the expected increase of polymerized tubulin, we propose that the cells may be attempting to compensate for the decreased microtubule stability by increasing MAP4 expression. The dynamic instability within a cell is crucial for cell function and proliferation. Many cells selected for resistance to microtubule-stabilizing drugs actually become dependent on the drug for survival [11, 32, 33, 44, 45]. This indicates that the microtubule alterations giving rise to the drug resistance are so dramatic that without external induction of microtubule polymerization, cell division cannot proceed. This is strongly supported by a recent study from Barlow et al. [46] that demonstrated that paclitaxel-dependent mutants have a substantial depletion in their levels of polymerized tubulin and require paclitaxel to stabilize the microtubules for cell division to proceed. In contrast, the dEpoB-resistant cells selected here have major changes in their microtubule system, but are not dependent on dEpoB for growth. It is highly feasible that the high MAP4 levels are compensating microtubule stability sufficiently for cell growth to occur in the absence of drug.

## Significance

Epothilones are a new class of tubulin-targeted agents that, like paclitaxel, can stabilize microtubules and arrest cells in mitosis. Our study has demonstrated that selection of acute lymphoblastic leukemia cells (CCRF-CEM) for resistance to the epothilone analog, desoxyepothilone B (dEpoB), has led to specific changes in the cellular target of this drug, resulting in reduced drug efficacy. Specifically, cells selected for resistance to 30, 60, and 140 nM dEpoB displayed reduced levels of polymerized tubulin indicative of less stable microtubules, counteracting the effects of the microtubule-stabilizing agent dEpoB. In contrast, these cells displayed hypersensitivity to microtubule-destabilizing agents. The reduction in polymerized tubulin is most likely due to an A231T mutation in class I  $\beta$ -tubulin in these cells. This mutation resides within helix 7 of  $\beta$ -tubulin, in a region implicated in controlling the conformation of the tubulin molecule. While this region is also defined as part of the paclitaxel binding pocket, the A231T mutation does not inhibit drug binding. In contrast, cells selected for higher level resistance (300 nM dEpoB) display markedly reduced drug binding. These cells have acquired an additional expressed mutation in class I  $\beta$ -tubulin, Q292E, near the M loop of  $\beta$ -tubulin, a region implicated in the lateral contacts of tubulin and microtubule stability. The tubulin in these cells fails to undergo drug-induced polymerization and displays ineffective [ $^3$ H]-paclitaxel

binding, suggesting that this residue is crucial for effective drug binding. This study identifies novel drug/target interactions, which improves our understanding of antimicrotubule drug action and may lead to improved antimicrotubule drug design.

## Experimental Procedures

### Cell Culture and Selection of Resistant Cells

Human T cell ALL cells, CCRF-CEM, and drug-resistant sublines were maintained in RPMI 1640 containing 10% FCS as suspension cultures. CCRF-CEM cells were selected by multiple stepwise treatments with increasing concentrations of dEpoB (kindly provided by Professor S. J. Danishefsky, Sloan-Kettering Institute for Cancer Research, New York). Initially cells were given  $4 \times 72$  hr doses of 30 nM dEpoB, after which the cells were able to grow through this treatment and designated dEpoB30. Cells were then treated  $3 \times 72$  hr at 60 nM dEpoB (designated dEpoB60),  $3 \times 72$  hr at 140 nM (designated dEpoB140), and  $5 \times 72$  hr at 300 nM dEpoB (designated dEpoB300) until no decreased viability was achieved at each of the respective concentrations. The resulting cell lines have since been maintained in drug-free media.

### Growth Inhibition Assays

Growth inhibition assays were performed as previously described [47]. Briefly, cells were seeded at 15,000 cells/well in 96-well plates in the presence or absence of the indicated drug concentrations. Cytotoxic drugs were obtained as follows: dEpoB, Dr. S. Danishefsky, Sloan-Kettering Institute for Cancer Research, NY; vinorelbine and vinflunine, Dr. B. Hill, Pierre Fabre, France; vincristine and colchicine (Sigma); vinblastine (David Bull Laboratories, Australia); doxorubicin (Pharmacia, Australia); epothilone B and paclitaxel (Calbiochem, San Diego, CA). After 72 hr incubation, metabolic activity was detected by addition of Alamar blue and spectrophotometric analysis. Cell numbers were determined and expressed as a percentage of control, untreated cells. Determination of  $IC_{50}$  values and statistical analysis was performed as described previously [48].

### MDR1 and MRP Gene Expression

PCR amplification of cDNA with specific primers for *MDR1* and *MRP1*, each with competitive amplification of  $\beta_2$ -microglobulin ( $\beta_2M$ ) as a control gene, were performed as previously described [49]. The products of triplicate PCR reactions were analyzed on polyacrylamide gels, and relative expression was determined by the densitometric volume of the *MDR1* or *MRP1* gene product in each cell line relative to that of the control  $\beta_2M$  gene. CEM/VCR-R cells, which have previously been shown to overexpress *MDR1* [48] and MCF7-VP16 cells, which have previously been shown to overexpress *MRP1* [50], were included as positive controls.

### Accumulation of [ $^3$ H]-Paclitaxel

The cellular accumulation of [ $^3$ H]-paclitaxel was performed as previously described [48]. Briefly, intracellular accumulation of paclitaxel was determined by adding [ $^3$ H]-paclitaxel (Moravek Biochemicals Inc., Brea, CA), to  $5 \times 10^6$  cells/1 ml in fresh growth medium and monitoring drug uptake over 1 hr. Mean incorporation was determined for duplicate 1 ml cultures to which [ $^3$ H]-paclitaxel (14.7 Ci/mmol; final concentration, 50 nM) was added. Cells were washed, hydrolyzed, and counted as previously described [48]. Mean incorporation of paclitaxel was determined for duplicate samples and expressed as pmoles of paclitaxel/mg protein. Three independent experiments were performed.

### Protein Expression Analysis

Total cellular proteins (10  $\mu$ g) were separated by 4%–15% SDS-PAGE and transferred to nitrocellulose as previously described [42]. Briefly, immunoblotting was performed using mAbs to class I  $\beta$ -tubulin (kind gift of Dr. Luduena, University of Texas, San Antonio, TX), class II  $\beta$ -tubulin, class III  $\beta$ -tubulin (Sigma), and MAP4 (Transduction Labs). Following incubation with a sheep anti-mouse horseradish-peroxidase-linked IgG antibody, membranes were developed using Supersignal (Pierce, Rockford, IL). Ponceau S staining



and a pAb to total actin (Sigma) were used to control for loading. Protein quantitation was performed on a Phosphorimager (Bio-Rad, Australia) and protein expression determined by dividing the densitometric value of the test protein by that of the control protein (actin). Statistical differences between the CEM cells and dEpoB-resistant cells were assessed using analysis of variance. All experiments were performed at least four times.

#### Measurement of Polymerized Tubulin

Soluble (cytosolic) and polymerized (cytoskeletal) fractions of tubulin were separated as previously described [42]. Briefly,  $2 \times 10^6$  cells were suspended in 100  $\mu$ l hypotonic buffer (1 mM  $MgCl_2$ , 2 mM EGTA, 0.5% NP-40, 2 mM phenylmethylsulfonyl fluoride, 10  $\mu$ l/ml protease inhibitor cocktail [Sigma], 20 mM Tris-HCl [pH 6.8]), incubated at 37°C for 5 min in the dark, and an additional 100  $\mu$ l buffer added. Polymerized tubulin was collected in the pellet following centrifugation at  $18,000 \times g$  for 10 min. Protein fractions were separated by SDS-PAGE and levels of tubulin determined by immunoblotting and detection using a mAb to  $\alpha$ -tubulin (Sigma). In addition, to assess the ability of dEpoB to induce tubulin polymerization in the resistant cell lines, 4  $\mu$ g/ml dEpoB was added to the hypotonic lysis buffer and the assay performed as above. All experiments were performed at least three times.

#### [<sup>3</sup>H]-Paclitaxel Binding Assay

Midlog phase cells were suspended at a final concentration of  $5 \times 10^6$  cells/ml in fresh RPMI/10% FCS. [<sup>3</sup>H]-paclitaxel (14.7 Ci/mmol; final concentration, 50 nM) was added to duplicate 1 ml cultures and incubated at 37°C for 1 hr. Cells were pelleted at  $2000 \times g$  for 1 min and washed thoroughly four times with warm (37°C) PBS. Soluble and polymerized fractions of tubulin were then separated as described above [42]. Protein concentration in each fraction was determined using the BCA assay (Pierce). The remaining sample was added to 2 ml scintillant (Ultima Gold; Packard, Australia) and radioactivity counted. Incorporation of paclitaxel in the polymerized fraction was determined for duplicate samples and expressed as pmoles of paclitaxel/mg protein. Experiments were performed in triplicate.

#### Sequencing of HM40 (Class I) $\beta$ -Tubulin Gene

Fluorescence cycle sequencing of the predominant  $\beta$ -tubulin iso-type gene, HM40 (class I), was performed in all cell lines on PCR-amplified cDNA using four overlapping primer sets as previously described [42]. dEpoB-resistant cell HM40 sequences were compared to the parental CEM cells and the published sequences [51, 52].

#### Two-Dimensional Polyacrylamide Gel Electrophoresis

CEM and dEpoB-resistant cells ( $1 \times 10^7$ ) were suspended in isoelectric focusing (IEF) buffer (7 M urea, 2 M thiourea, 2% CHAPS, 1% sulfobetaines 3–10, 1% amidosulfobetaine-14, 2 mM tributyl phosphine, 65 mM dithiothreitol, 1% carrier ampholytes 3–10, 1% carrier ampholytes 4–6, 0.01% bromophenol blue) to a final concentration of 1 mg/ml as determined by amino acid analysis [53]. Cells were lysed by pulse sonication twice on ice. Endonuclease (Sigma) (1 U/ $\mu$ g protein) was added and incubated at room temperature for 30 min. Protein extracts were centrifuged at  $18,000 \times g$  for 12 min and the supernatant collected. Narrow range immobilized pH gradient (IPG) strips, pH 4.5–5.5 (Pharmacia, Sweden), were rehydrated in 500  $\mu$ l IEF buffer. Protein (100  $\mu$ g) was cup-loaded and IEF performed for 150,000Vhr on a Multiphor II apparatus (Pharmacia). Second dimension SDS-PAGE was performed in 10%–14%T polyacrylamide gels as previously described [54]. Gels were stained with SYPRO Ruby (Bio-Rad) according to the manufacturers instructions and visualized on a Molecular Imager FX (Bio-Rad), or transferred to nitrocellulose using standard methods [55] and tubulin isotypes detected using mAbs as described above.

#### MALDI-TOF Mass Spectrometry

Spots were excised from SYPRO Ruby stained gels, washed twice in 25 mM  $NH_4HCO_3$ , 50% acetonitrile, spun dry, and in-gel trypsin digested in 10 ng/ $\mu$ l trypsin (Promega) in 25 mM  $NH_4HCO_3$  for 16 hr at 37°C. Peptides were extracted from the gel with 50% (v/v) acetonitrile, 1% (v/v) TFA solution. A 1  $\mu$ l aliquot was spotted onto

a sample plate with 1  $\mu$ l of matrix ( $\alpha$ -cyano-4-hydroxycinnamic acid, 8 mg/ml in 50% v/v AcN, 1% v/v TFA). Matrix-assisted laser desorption ionization-time of flight (MALDI-TOF) mass spectrometry acquisition was performed on a ToFSpec 2E mass spectrometer (Micromass, Manchester, UK) set to reflectron mode. Known trypsin autocleavage peptide masses (842.51 Da; 2211.10 Da) were used for a 2-point internal calibration for each spectrum. Peptide masses were searched against SwissProt/TrEMBL protein databases using the PeptIdent tool on ExPASy (<http://tw.expasy.org/tools/peptident.html>) for protein identification.

#### ESI-TOF Tandem Mass Spectrometry

Upon analysis of MALDI-TOF mass spectra, class I  $\beta$ -tubulin peptides differing in mass between the parental CEM cells and drug-resistant cells were selected for amino acid sequencing by ESI-TOF MS/MS. After in-gel trypsin digestion, the peptides were purified using a porous R2 resin column [56]. The sample was then analyzed by ESI-TOF MS/MS using a Micromass Q-TOF MS and data manually acquired using borosilicate capillaries for nanospray acquisition. Data was acquired over the m/z range 400–1800 Da to select peptides for MS/MS analysis. After peptides were selected, the MS was switched to MS/MS mode and data collected over the m/z range 50–2000 Da with variable collision energy settings. The peptide sequences were compared to the parental CEM cells and the published sequences [51, 52].

#### Tubulin Mutation Modeling

Computer models of the locations of mutations identified within  $\beta$ -tubulin of dEpoB-resistant cells were prepared using the ViewerLite program from Accelrys. Coordinates for wild-type  $\beta$ -tubulin were obtained from the Protein Data Bank (PDB accession code: 1JFF). Mutated proteins were created using the MUTATE command within SWISS PDB viewer.

#### Acknowledgments

The authors would like to thank Professor S.J. Danishefsky, Sloan-Kettering Institute for Cancer Research, New York for kindly providing the dEpoB; Dr. B. Hill, Pierre Fabre, France for supplying the vinorelbine and vinflunine; and Dr. M. Larsen, University of Aarhus, Denmark for assistance with ESI-TOF operation. This work was supported by the Children's Cancer Institute Australia for Medical Research, which is affiliated with the University of New South Wales and Sydney Children's Hospital. This project was supported by grants from the National Health and Medical Research Council, New South Wales Cancer Council, and Cure Cancer Australia Foundation. Ms. Verrills is supported by an Australian Postgraduate Award. This research has been facilitated by access to the Australian Proteome Analysis Facility established under the Australian Government's Major National Research Facilities Program.

Received: March 1, 2003

Revised: May 8, 2003

Accepted: May 13, 2003

Published: July 18, 2003

#### References

1. Eisenhauer, E.A., and Vermorken, J.B. (1998). The taxoids. Comparative clinical pharmacology and therapeutic potential. *Drugs* 55, 5–30.
2. Downing, K.H. (2000). Structural basis for the interaction of tubulin with proteins and drugs that affect microtubule stability. *Annu. Rev. Cell Dev. Biol.* 16, 89–111.
3. Horwitz, S.B. (1992). Mechanism of action of taxol. *Trends Pharmacol. Sci.* 13, 134–136.
4. Jordan, M.A., Toso, R.J., Thrower, D., and Wilson, L. (1993). Mechanism of mitotic block and inhibition of cell proliferation by taxol at low concentrations. *Proc. Natl. Acad. Sci. USA* 90, 9552–9556.
5. Stachel, S.J., Biswas, K., and Danishefsky, S.J. (2001). The epothilones, eleutherobins, and related types of molecules. *Curr. Pharm. Des.* 7, 1277–1290.
6. Kavallaris, M., Verrills, N.M., and Hill, B.T. (2001). Anticancer

- therapy with novel tubulin-interacting drugs. *Drug Resist. Updat.* **4**, 392–401.
7. Bollag, D.M., McQueney, P.A., Zhu, J., Hensens, O., Koupal, L., Liesch, J., Goetz, M., Lazarides, E., and Woods, C.M. (1995). Epothilones, a new class of microtubule-stabilizing agents with a taxol-like mechanism of action. *Cancer Res.* **55**, 2325–2333.
  8. Kowalski, R.J., Giannakakou, P., and Hamel, E. (1997). Activities of the microtubule-stabilizing agents epothilones A and B with purified tubulin and in cells resistant to paclitaxel (Taxol(R)). *J. Biol. Chem.* **272**, 2534–2541.
  9. Ojima, I., Chakravarty, S., Inoue, T., Lin, S., He, L., Horwitz, S.B., Kuduk, S.D., and Danishefsky, S.J. (1999). A common pharmacophore for cytotoxic natural products that stabilize microtubules. *Proc. Natl. Acad. Sci. USA* **96**, 4256–4261.
  10. He, L., Jagtap, P.G., Kingston, D.G., Shen, H.J., Orr, G.A., and Horwitz, S.B. (2000). A common pharmacophore for Taxol and the epothilones based on the biological activity of a taxane molecule lacking a C-13 side chain. *Biochemistry* **39**, 3972–3978.
  11. Giannakakou, P., Gussio, R., Nogales, E., Downing, K.H., Zaharevitz, D., Bollbuck, B., Poy, G., Sackett, D., Nicolaou, K.C., and Fojo, T. (2000). A common pharmacophore for epothilone and taxanes: molecular basis for drug resistance conferred by tubulin mutations in human cancer cells. *Proc. Natl. Acad. Sci. USA* **97**, 2904–2909.
  12. Giannakakou, P., Sackett, D.L., Kang, Y.K., Zhan, Z., Buters, J.T., Fojo, T., and Poruchynsky, M.S. (1997). Paclitaxel-resistant human ovarian cancer cells have mutant beta-tubulins that exhibit impaired paclitaxel-driven polymerization. *J. Biol. Chem.* **272**, 17118–17125.
  13. Chou, T.C., Zhang, X.G., Balog, A., Su, D.S., Meng, D., Savin, K., Bertino, J.R., and Danishefsky, S.J. (1998). Desoxyepothilone B: an efficacious microtubule-targeted antitumor agent with a promising in vivo profile relative to epothilone B. *Proc. Natl. Acad. Sci. USA* **95**, 9642–9647.
  14. Chou, T.C., Zhang, X.G., Harris, C.R., Kuduk, S.D., Balog, A., Savin, K.A., Bertino, J.R., and Danishefsky, S.J. (1998). Desoxyepothilone B is curative against human tumor xenografts that are refractory to paclitaxel. *Proc. Natl. Acad. Sci. USA* **95**, 15798–15802.
  15. Lee, F.Y., Borzilleri, R., Fairchild, C.R., Kim, S.H., Long, B.H., Reventos-Suarez, C., Vite, G.D., Rose, W.C., and Kramer, R.A. (2001). BMS-247550: a novel epothilone analog with a mode of action similar to paclitaxel but possessing superior antitumor efficacy. *Clin. Cancer Res.* **7**, 1429–1437.
  16. McDaid, H.M., Mani, S., Shen, H., Muggia, F., Sonnichsen, D., and Horwitz, S.B. (2002). Validation of the pharmacodynamics of BMS-247550, an analogue of epothilone B, during phase I clinical study. *Clin. Cancer Res.* **8**, 2035–2043.
  17. Chou, T.C., O'Connor, O.A., Tong, W.P., Guan, Y., Zhang, Z.G., Stachel, S.J., Lee, C., and Danishefsky, S.J. (2001). The synthesis, discovery, and development of a highly promising class of microtubule stabilization agents: curative effects of desoxyepothilones B and F against human tumor xenografts in nude mice. *Proc. Natl. Acad. Sci. USA* **98**, 8113–8118.
  18. Dumontet, C. (2000). Mechanisms of action and resistance to tubulin-binding agents. *Expert Opin. Investig. Drugs* **9**, 779–788.
  19. Burkhart, C.A., Kavallaris, M., and Horwitz, S.B. (2001). The role of  $\beta$ -tubulin isotypes in resistance to antimetabolic drugs. *Biochim. Biophys. Acta* **1471**, 1–9.
  20. Drukman, S., and Kavallaris, M. (2002). Microtubule alterations and resistance to tubulin-binding agents. *Int. J. Oncol.* **21**, 621–628.
  21. Zhang, C.C., Yang, J.M., White, E., Murphy, M., Levine, A., and Hait, W.N. (1998). The role of MAP4 expression in the sensitivity to paclitaxel and resistance to vinca alkaloids in p53 mutant cells. *Oncogene* **16**, 1617–1624.
  22. Nguyen, H.L., Chari, S., Gruber, D., Lue, C.M., Chapin, S.J., and Bulinski, J.C. (1997). Overexpression of full- or partial-length MAP4 stabilizes microtubules and alters cell growth. *J. Cell Sci.* **110**, 281–294.
  23. Nogales, E., Wolf, S.G., and Downing, K.H. (1998). Structure of the  $\alpha\beta$  tubulin dimer by electron crystallography. *Nature (Lond.)* **391**, 199–203.
  24. Meurer-Grob, P., Kasparian, J., and Wade, R.H. (2001). Microtubule structure at improved resolution. *Biochemistry* **40**, 8000–8008.
  25. Rao, S., Orr, G.A., Chaudhary, A.G., Kingston, D.G.I., and Horwitz, S.B. (1995). Characterization of the taxol binding site on the microtubule. 2-(m-Azidobenzoyl)taxol photolabels a peptide (amino acids 217–231) of beta-tubulin. *J. Biol. Chem.* **270**, 20235–20238.
  26. Amos, L.A., and Lowe, J. (1999). How Taxol stabilises microtubule structure. *Chem. Biol.* **6**, R65–R69.
  27. Amos, L.A. (2000). Focusing-in on microtubules. *Curr. Opin. Struct. Biol.* **10**, 236–241.
  28. Derry, W.B., Wilson, L., and Jordan, M.A. (1995). Substoichiometric binding of taxol suppresses microtubule dynamics. *Biochemistry* **34**, 2203–2211.
  29. Minotti, A.M., Barlow, S.B., and Cabral, F. (1991). Resistance to antimetabolic drugs in Chinese hamster ovary cells correlates with changes in the level of polymerized tubulin. *J. Biol. Chem.* **266**, 3987–3994.
  30. Snyder, J.P., Nettles, J.H., Cornett, B., Downing, K.H., and Nogales, E. (2001). The binding conformation of Taxol in beta-tubulin: a model based on electron crystallographic density. *Proc. Natl. Acad. Sci. USA* **98**, 5312–5316.
  31. Nogales, E., Whittaker, M., Milligan, R.A., and Downing, K.H. (1999). High-resolution model of the microtubule. *Cell* **96**, 79–88.
  32. Gonzalez-Garay, M.L., Chang, L., Blade, K., Menick, D.R., and Cabral, F. (1999). A beta-tubulin leucine cluster involved in microtubule assembly and paclitaxel resistance. *J. Biol. Chem.* **274**, 23875–23882.
  33. He, L., Yang, C.-P.H., and Horwitz, S.B. (2001). Mutations in B-tubulin map to domains involved in regulation of microtubule stability in epothilone-resistant cell lines. *Mol. Cancer Ther.* **1**, 3–10.
  34. Haber, M., Burkhart, C.A., Regl, D.L., Madafiglio, J., Norris, M.D., and Horwitz, S.B. (1995). Altered expression of M beta 2, the class II beta-tubulin isotype, in a murine J774.2 cell line with a high level of taxol resistance. *J. Biol. Chem.* **270**, 31269–31275.
  35. Kavallaris, M., Kuo, D.Y., Burkhart, C.A., Regl, D.L., Norris, M.D., Haber, M., and Horwitz, S.B. (1997). Taxol-resistant epithelial ovarian tumors are associated with altered expression of specific beta-tubulin isotypes. *J. Clin. Invest.* **100**, 1282–1293.
  36. Luduena, R.F. (1998). Multiple forms of tubulin: different gene products and covalent modifications. *Int. Rev. Cytol.* **178**, 207–275.
  37. McKean, P.G., Vaughan, S., and Gull, K. (2001). The extended tubulin family. *J. Cell Sci.* **114**, 2723–2733.
  38. Rosenbaum, J. (2000). Cytoskeleton: functions for tubulin modifications at last. *Curr. Biol.* **10**, R801–R803.
  39. Derry, W.B., Wilson, S., Khan, I.A., Luduena, R.F., and Jordan, M.A. (1997). Taxol differentially modulates the dynamics of microtubules assembled from unfractionated and purified  $\beta$ -tubulin isotypes. *Biochemistry* **36**, 3554–3562.
  40. Lu, Q., and Luduena, R.F. (1993). Removal of BIII isotype enhances taxol induced microtubule assembly. *Cell Struct. Funct.* **18**, 173–182.
  41. Kavallaris, M., Burkhart, C.A., and Horwitz, S.B. (1999). Antisense oligonucleotides to class III beta-tubulin sensitize drug-resistant cells to Taxol. *Br. J. Cancer* **80**, 1020–1025.
  42. Kavallaris, M., Tait, A.S., Walsh, B.J., He, L., Horwitz, S.B., Norris, M.D., and Haber, M. (2001). Multiple microtubule alterations are associated with Vinca alkaloid resistance in human leukemia cells. *Cancer Res.* **61**, 5803–5809.
  43. Nguyen, H.L., Gruber, D., and Bulinski, J.C. (1999). Microtubule-associated protein 4 (MAP4) regulates assembly, protomer-polymer partitioning and synthesis of tubulin in cultured cells. *J. Cell Sci.* **112**, 1813–1824.
  44. Martello, L.A., McDaid, H.M., Regl, D.L., Yang, C.P., Meng, D., Pettus, T.R., Kaufman, M.D., Arimoto, H., Danishefsky, S.J., Smith, A.B., III, and Horwitz, S.B. (2000). Taxol and discodermolide represent a synergistic drug combination in human carcinoma cell lines. *Clin. Cancer Res.* **6**, 1978–1987.
  45. Martello, L.A., Verdier-Pinard, P., Shen, H.-J., He, L., Orr, G.A., and Horwitz, S.B. (2003). Elevated levels of microtubule destabi-

- lizing factors in a Taxol-resistant/dependent A549 cell line with an  $\alpha$ -tubulin mutation. *Cancer Res.* 63, 1207–1213.
46. Barlow, S.B., Gonzalez-Garay, M.L., and Cabral, F. (2002). Paclitaxel-dependent mutants have severely reduced microtubule assembly and reduced tubulin synthesis. *J. Cell Sci.* 115, 3469–3478.
  47. Gifford, A.J., Kavallaris, M., Madafiglio, J., Matherly, L.H., Stewart, B.W., Haber, M., and Norris, M.D. (1998). P-glycoprotein-mediated methotrexate resistance in CCRF-CEM sublines deficient in methotrexate accumulation due to a point mutation in the reduced folate carrier gene. *Int. J. Cancer* 79, 176–181.
  48. Haber, M., Norris, M.D., Kavallaris, M., Bell, D.R., Davey, R.A., White, L., and Stewart, B.W. (1989). Atypical multidrug resistance in a therapy-induced drug resistant human leukemia cell line (LALW-2): resistance to vinca alkaloids is independent of P-glycoprotein. *Cancer Res.* 49, 5281–5287.
  49. Bordow, S.B., Haber, M., Madafiglio, J., Cheung, B., Marshall, G.M., and Norris, M.D. (1994). Expression of the multidrug resistance-associated protein (*MRP*) gene correlates with amplification and overexpression of the *N-myc* oncogene in childhood neuroblastoma. *Cancer Res.* 54, 5036–5040.
  50. Schneider, E., Horton, J.K., Yang, C.H., Nakagawa, M., and Cowan, K.H. (1994). Multidrug resistance-associated protein gene overexpression and reduced drug sensitivity of topoisomerase II in a human breast carcinoma MCF7 cell line selected for etoposide resistance. *Cancer Res.* 54, 152–158.
  51. Cowan, N.J., and Dudley, L. (1983). Tubulin isotypes and the multigene tubulin families. *Int. Rev. Cytol.* 85, 147–173.
  52. Lee, M.G., Lewis, S.A., Wilde, C.D., and Cowan, N.J. (1983). Evolutionary history of a multigene family: an expressed human beta-tubulin gene and three processed pseudogenes. *Cell* 33, 477–487.
  53. Cordwell, S.J., Wilkins, M.R., Cerpa-Poljak, A., Gooley, A.A., Duncan, M., Williams, K.L., and Humphery-Smith, I. (1995). Cross-species identification of proteins separated by two-dimensional gel electrophoresis using matrix-assisted laser desorption ionisation/time-of-flight mass spectrometry and amino acid composition. *Electrophoresis* 16, 438–443.
  54. Verrills, N.M., Harry, J.H., Walsh, B.J., Hains, P.G., and Robinson, E.S. (2000). Cross-matching marsupial proteins with eutherian mammal databases: proteome analysis of cells from UV-induced skin tumours of an opossum (*Monodelphis domestica*). *Electrophoresis* 21, 3810–3822.
  55. Towbin, H., Staehelin, T., and Gordon, J. (1979). Electrophoretic transfer of proteins from nitrocellulose sheets: procedure and some applications. *Proc. Natl. Acad. Sci. USA* 76, 4350–4354.
  56. Larsen, M.R., Larsen, P.M., Fey, S.J., and Roepstorff, P. (2001). Characterization of differently processed forms of enolase 2 from *Saccharomyces cerevisiae* by two-dimensional gel electrophoresis and mass spectrometry. *Electrophoresis* 22, 566–575.